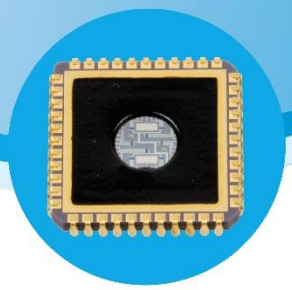

Towards Novel Graphene-Enabled Diagnostic Assays with Improved Signal to Noise Ratio

Savannah J. Afsahi, Lauren E. Locascio, Deng Pan, PhD, Yingning Gao, PhD, Amy E. Walker, Francie E. Barron, PhD, Brett R. Goldsmith, PhD, Mitchell B. Lerner, PhD

This is a pre-print of a paper that has been published in a scientific journal:

Afsahi, *et. al*., Towards Novel Graphene-Enabled Diagnostic Assays with Improved Signal to Noise Ratio, MRS Advances (2017), DOI: 10.1557/adv.2017.431

ABSTRACT

Large numbers of high quality graphene transistors were fabricated by chemical vapor deposition and packaged into a standard electronics assembly, enabling the readout of graphene properties on the benchtop. After chemical functionalization, these sensors demonstrate sensitivity into the pM range to inflammation (IL6) and Zika virus (ZIKV NS1) biomarkers. Signal to noise ratio (SNR) of graphene biosensors is over an order of magnitude greater than established diagnostic and biophysical assays, namely ELISA and BLI respectively. High precision measurements of protein kinetics captured using this technology, commercially available as the AGILE R100, are comparable to both clinical diagnostic and state-of-the-art biomolecule characterization tools. These results demonstrate that graphene-based platforms are highly attractive biological sensors for next generation diagnostics.

INTRODUCTION

Characterization of binding interactions is critical in all stages of clinical and research based disease intervention.[1] Accurate early stage diagnosis can significantly improve patient outcomes and reduce medical costs.[2] The current generation of antibody based diagnostic tools, such as enzyme-linked immunosorbent assays (ELISA), struggle in detecting disease biomarkers due to interfering compounds in biological fluids.[3] Characterization of binding kinetics is also a key metric in development of novel biotherapeutics. Current biophysical assays such as Bio-Layer Interferometry (BLI) are costly and labor intensive.[4] Both clinical and biophysical antibody binding assays demonstrate noise interference at ultralow concentrations, resulting in reduced sensitivity.[5] Noise interference lengthens the time to diagnosis in clinical assays and inhibits characterization of binding kinetics at physiological or therapeutic levels in biophysical analysis,[6] thus complicating development of biotherapeutics.[7] Next-generation biosensors must increase their signal-to-noise ratio (SNR) to detect biomarkers in low levels and complex background to drive biotherapeutic advances in clinical and research applications.[8,9]

Highly sensitive nanomaterials have been investigated as biosensors for decades. Graphene is a two-dimensional sheet of hexagonally arranged carbon atoms with the highest room temperature carrier mobility of any material and extremely low electronic noise.[9] Every atom in a graphene sheet is in direct contact with its environment, making it an ideal candidate for sensing applications.[10] Graphene has been incorporated into sensors of all varieties, including pressure,[11] vapor,[8,12] optical,[13] and biomolecular sensors.[14] We have demonstrated a commercially mass-produced graphene biosensor read out by low-cost, portable electronic hardware.[15] That platform is applied here in detecting inflammatory and viral biomarker proteins, namely human recombinant interleukin 6 (IL-6) and Zika virus (ZIKV NS1) respectively. When compared to clinical and research characterization methods for IL-6 and ZIKV NS1, the graphene biosensor demonstrates much higher SNR than ELISA and BLI respectively.

The graphene biosensor chip relies on Field Effect Biosensing (FEB) technology. FEB measures the channel current and gate capacitance of a graphene field effect transistor (FET) with biological targets immobilized on the surface serving as the gate dielectric. Unlike an FET, an FEB biosensor has no oxide or other dielectric in between the conduction channel and the biological material under test. As previously described, FEB biosensors use a liquid gate precisely controlled by Pt reference and counter electrodes.[15] A small bias is also placed across the graphene itself, and the current through the graphene is then measured while the liquid gate is altered. The resulting channel current versus liquid gate transfer curve is simplified to 2 values: the

percent change in the average current response across the entire gate sweep (I-Response) and the percent change in the average slope of the transfer curve (C-Response).[15] Voltages are kept small (≤100 mV) to avoid direct charge transfer or electrochemistry with the graphene.

FEB-based biosensors have been in limited use in laboratory environments for several years and are advantageous over other electrobiochemical sensors in terms of sensitivity, selectivity, response time, and ease of fabrication.[16–18] Furthermore, graphene FEB biosensors show low levels of thermal and electrical noise due to the high conductivity and crystal structure of graphene.[16] A schematic of the AGILE R100 reader with a graphene biosensor chip is shown in Figure 1a. Interactions and binding events with the analyte change source-drain current and transconductance, enabling accurate and label-free kinetic, affinity, and concentration measurements in real-time. A microscope image of the chip surface is presented in Figure 1b. Eight sets of 5 graphene channels are exposed for antibody immobilization and target analyte interrogation while the rest of the chip surface is passivated with insulating material. On-chip reference and counter electrodes provide the liquid gate voltage that drives the biochemistry.

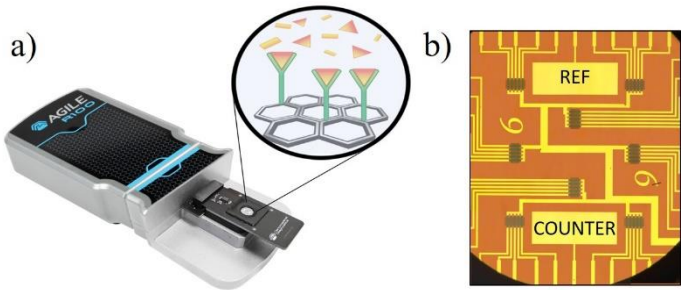

Figure 1. a) AGILE R100 System and illustration depicting binding of immobilized capture molecules to free-floating analyte. Image reprinted with permission from Nanomedical Diagnostics. b) Optical microscope image of sensor surface composed of graphene channels, Pt source/drain contacts, and Pt reference and counter electrodes.

MATERIALS AND METHODS

Fabrication of AGILE R100 Graphene Biosensors

Biosensor chips are fabricated at a commercial MEMS foundry using conventional processing techniques as described in previous literature.[15] Briefly, Ti/Pt source, drain, and reference electrodes are patterned on 6" silicon wafers using a liftoff process with thorough cleaning. High quality graphene films are grown in tube furnaces at temperatures exceeding 1030 °C on copper foil (Alfa Aesar) by catalytic decomposition of methane gas.[19] Graphene films are transferred from the copper foil growth substrate to the target wafer by bubbling transfer as described in the literature.[20] Finally, graphene sheets are patterned into defined channels between the source-drain electrodes, and then the metal contacts to the graphene are passivated with a plasma-enhanced CVD silicon oxide layer.

Anti-IL6 Immobilization with EDC/sNHS on Graphene Biosensors

The AGILE R100 biosensor chips were treated with 4-carboxy-benzene diazonium tetrafluoroborate for 30 min at 40 °C, washed in 100% isopropanol and dried with nitrogen. Additionally, 1-pyrene carboxylic acid in 100% methanol was applied to the chips to functionalize the surface with carboxyl groups. The sensor was calibrated to baseline in 50 mM 2-(*N*-Morpholino) ethanesulfonic acid (MES) pH 6.0 (VWR) for 60 s. Then, a solution containing 5 mL 50 mM MES pH 6.0, 2 mg 1-ethyl-3-(3-dimethylaminopropyl)carbodiimide (EDC; VWR), and 6 mg *N*-hydroxysulfosuccinimide (sNHS; G-Biosciences) was mixed and immediately added to each chip for 15 min. The chips were rinsed in 50 mM MES pH 6.0.

Human monoclonal antibody to Interleukin 6 (anti-IL6; Invitrogen) was diluted to 14.6 nM in 1X phosphate buffered saline (PBS) pH 7.4 and immobilized on the surface over a period of 15 min. Residual amine-reactive sNHS ester groups were subsequently quenched using 3 mM amino-PEG5-alcohol solution pH 7.4 (BroadPharm) and 1 M Ethanolamine pH 8.5 for 15 min. Each analyte concentration was prepared in 1X PBS pH 7.4 and was applied for 10 min to detect analyte association (k_a). The I- and C-Response were measured and used in kinetic analysis. The resulting concentration of immobilized capture molecules on the biosensor chip surface is approximately 5 antibodies per square micron.[14] The graphene biosensor surface is functionalized such that reactive NHS esters may crosslink with free amines on protein residues throughout the immobilized molecule structure.

Anti-Zika NS1 Immobilization with Pyrene-bNHS on Graphene Biosensors

A 1 mM solution of 1-Pyrenebutyric acid *N*-hydroxysuccinimide ester (Pyrene-bNHS; Sigma Aldrich) was prepared in 100% methanol. The AGILE R100 biosensor chips were covered in 10 mL 1 mM Pyrene-bNHS solution and incubated in a sealed container for 2 hrs at room temperature. The biosensor chips were then rinsed for 5 min in 10 mL 100% methanol and dried with nitrogen. 75 µL of all solutions was used and incubation steps took place at room temperature.

Anti-Zika NS1 mouse monoclonal was diluted to a working concentration of 14.6 nM in 1X PBS pH 7.4 and applied to the biosensor chip surface. Further antibody immobilization followed the standard procedures listed previously. The ZIKV NS1 recombinant antigen (The Native Antigen Ltd) was diluted in 1X PBS pH 7.4 to concentrations of 18 ng/mL, 56 ng/mL, 166 ng/mL, and 500 ng/mL. The C-Response was measured and used in kinetic analysis.

Label-free BLI analysis on Octet Red96 (Forte Bio) was performed in kinetic buffer (PBS/0.05% BSA/0.02% Tween20), using anti-mouse Fc (AMC) biosensors. Biosensors were equilibrated for 10 min in kinetic buffer. Microplates were then filled with 200 µl of sample in kinetic buffer and

agitated at 1000 rpm. Biosensors were loaded with 1-2 µg anti-Zika NS1 for a response of 0.5 to 0.8 ± 0.15 nm among 8 sensors. A 7-point titration curve of binding to ZIKV NS1 (700 nM to 2.9 nM) with subtracted buffer reference was performed for 1000 s and buffer dissociated for 2000 s. Data was analyzed in Octet Data Analysis 9.0 software.

RESULTS AND DISCUSSION

Antibody Immobilization on Graphene Biosensors

Covalent linkage of the antibody on the chip surface is measured in real-time using custom software. The size and charge profile of the antibody affect the I-Response and C-Response of the sensor. Blocking and quenching steps prevent nonspecific covalent protein attachment to the surface, reducing noise during sensing and enabling specific detection in complex samples. Binding of a charged analyte to an immobilized antibody generates electrical changes at the graphene surface that can be read out electronically. Figure 2a shows the C-Response of the biosensor chip throughout the functionalization process. Notably, anti-IL6 antibody immobilization produced a 20% increase in the C-Response. Figure 2b shows the I-Response during IL6 detection at 50 pM and subsequent IL6 release from immobilized anti-IL6 upon rinsing. At this concentration, the maximum I-Response is ~9%, significantly above the noise floor of the graphene biosensor (<0.2%). The association and disassociation curves measured here are expected for an antibody-antigen interaction.[21]

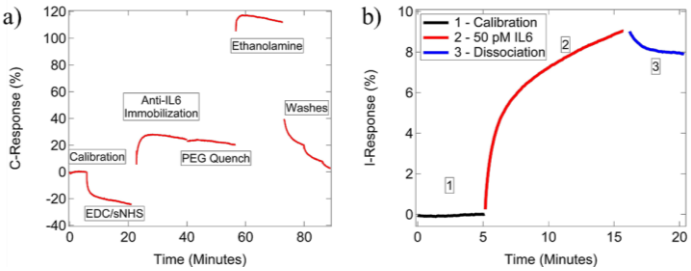

Figure 2. (a) C-Response throughout anti-IL6 immobilization and quenching on graphene biosensor chip. (b) Sensing and dissociation of 50 pM IL6 from immobilized anti-IL6.

Signal-to-Noise Comparison of Field Effect Biosensing and Enzyme Linked Immunosorbent Assay

Maximizing sensitivity and selectivity is critical for diagnostic tests. Sensitivity of an assay can be evaluated using the SNR, where a larger SNR allows for more accurate quantification at low concentrations. Lower limits of detection (LLOD) enable earlier medical intervention and improved clinical outcomes. The noise response of the system is the average signal generated by a blank sample (0 nM of analyte). Sensitivity of IL6 detection on graphene biosensors was determined by running multiple concentrations of the analyte to determine the LLOD, defined as the concentration where SNR is greater than 3 for the I-Response data channel.

IL6 ELISA binding data is reported from the Invitrogen Human IL6 ELISA Kit Product Information Sheet. Figure 3 shows the SNR over a wide range of concentrations of IL6 for both the AGILE R100 assay and commercial IL6 ELISA assay. The LLOD for the AGILE R100 assay was calculated at 0.1 pM, and the LLOD for the ELISA assay was calculated at 6 pM. Using either the LLOD or the SNR at a given concentration for each assay type, the AGILE R100 outperforms the ELISA assay by over a factor of 10.

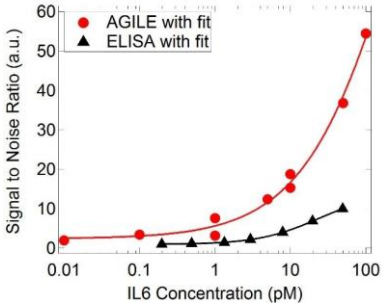

Figure 3. SNR data comparison of detection of recombinant IL6 using anti-IL6 monoclonal antibody with ELISA versus AGILE R100 I-Response data.

Signal-to-Noise Comparison of Field Effect Biosensing and Bio-Layer Interferometry

Sensitivity of ZIKV NS1 detection on an FEB system recording I-Response and a BLI system (Figure 4a) was determined by running several concentrations of the analyte to determine the LLOD and evaluate the binding kinetics. The LLOD on the BLI system was calculated at 1.4 nM while the LLOD on AGILE R100 was determined to be 0.45 nM, indicating that FEB is more sensitive at detecting ZIKV NS1 than BLI. Additionally, a plot of SNR versus analyte concentration (Figure 4b) shows that over a range of concentrations, AGILE R100 biosensor chips have a greater SNR, indicating that FEB signal is more robust and easier to detect than BLI signal.

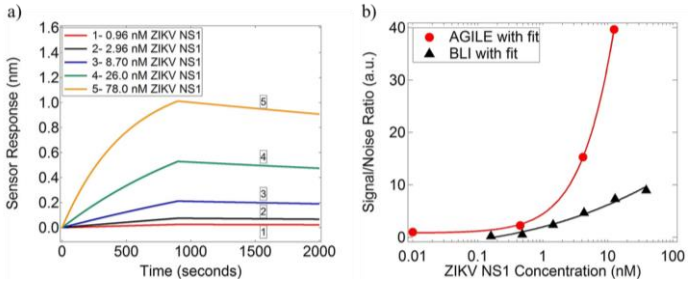

Figure 4. (a) Sensorgrams of anti-Zika NS1 in response to various concentrations of ZIKV NS1 on a BLI system. The LLOD is 1.4 nM. (b) SNR versus ZIKV NS1 concentration on FEB (I-Response) and BLI systems.

AGILE R100 Biosensor Chips, like BLI sensors, generate accurate, real-time kinetic data. Association of ZIKV NS1 to immobilized anti-Zika NS1 was quantified using the Hill-Langmuir model of saturable kinetic binding on both FEB and BLI platforms. The resulting association rates (k_a) were 2.97×10^4 Ms^{-1} on a BLI tool and 9.27×10^4 Ms^{-1} on AGILE R100. These association rates agree within error, indicating that graphene biosensors generate kinetic data comparable to more expensive and laborious biophysical assays such as BLI without compromising accuracy.

CONCLUSIONS

Quantitative studies on the sensitivity of graphene-enabled biosensors in solution are reported and compared to commonly used assays. Our results show that graphene biosensors are highly advantageous for chemical and biological detection due to the low electrical noise in graphene. The SNR of graphene devices was demonstrated to be nearly an order of magnitude greater at a given analyte molecule concentration compared to ELISA (IL6 biomarker assay) and BLI (Zika biomarker assay), demonstrating graphene biosensor efficacy in research sectors with projected clinical diagnostic improvements. The LLOD for both the IL6 and ZIKV NS1 analytes were also improved by over 10x using the AGILE R100 system. In addition to the high sensitivity of the graphene platform, field effect biosensing of ZIKV NS1 generates biophysical kinetic data in agreement with BLI. Overall, the AGILE R100 represents a single platform that could be used across the drug and diagnostic development pipeline to reduce costly data and procedure translations due to its capabilities lowering LOD and increasing SNR at ultralow concentrations. Graphene biosensors have the potential to accelerate clinical application of biotherapeutic products to the healthcare market with the goal of benefiting patients in critical need.

ACKNOWLEDGMENTS

We would like to acknowledge Dr. Jason Goldstein and Dr. Jolie Nokes for their assistance on this project. This research did not receive any specific grant from funding agencies in the public, commercial, or not-for-profit sectors.

REFERENCES

1. Borrebaeck CAK. Antibodies in diagnostics - From immunoassays to protein chips. *Immunol Today*. 2000;21(8):379-382. doi:10.1016/S0167-5699(00)01683-2.
2. Graber M, Gordon R, Franklin N. Reducing diagnostic errors in medicine: what's the goal? *Acad Med*. 2002;77(10):981-992. doi:10.1097/00001888-200210000-00009.
3. Findlay JWA, Smith WC, Lee JW, et al. Validation of immunoassays for bioanalysis: A pharmaceutical industry perspective. *J Pharm Biomed Anal*. 2000;21(6):1249-1273. doi:10.1016/S0731-7085(99)00244-7.
4. McGlennen RC. Miniaturization technologies for molecular diagnostics. *Clin Chem*. 2001;47(3):393-402.
5. Mire-Sluis a R, Barrett YC, Devanarayan V, et al. Recommendations for the design and optimization of immunoassays used in the detection of host antibodies against biotechnology products. *J Immunol Methods*. 2004;289(1-2):1-16. doi:10.1016/j.jim.2004.06.002.
6. Gonzalez RM, Seurynck-Servoss SL, Crowley SA, et al. Development and validation of sandwich Elisa microarrays with minimal assay interference. *J Proteome Res*. 2008;7(6):2406-2414. doi:10.1021/pr700822t.
7. Tetin SY, Stroupe SD. Antibodies in diagnostic applications. *Curr Pharm Biotechnol*. 2004;5(1):9-16. doi:10.2174/1389201043489602.
8. Lu Y, Goldsmith BR, Kybert NJ, Johnson ATC. DNA-decorated graphene chemical sensors. *Appl Phys Lett*. 2010;97(8). doi:10.1063/1.3483128.
9. Choi W, Lahiri I, Seelaboyina R, Kang YS. Synthesis of Graphene and Its Applications: A Review. *Crit Rev Solid State Mater Sci*. 2010;35(1):52-71. doi:10.1080/10408430903505036.
10. Zhan B, Li C, Yang J, Jenkins G, Huang W, Dong X. Graphene field-effect transistor and its application for electronic sensing. *Small*. 2014;10(20):4042-4065. doi:10.1002/smll.201400463.
11. Zhu SE, Krishna Ghatkesar M, Zhang C, Janssen GCAM. Graphene based piezoresistive pressure sensor. *Appl Phys Lett*. 2013;102(16). doi:10.1063/1.4802799.
12. Esfandiar A, Kybert NJ, Dattoli EN, et al. DNA-decorated graphene nanomesh for detection of chemical vapors. *Appl Phys Lett*. 2013;103(18). doi:10.1063/1.4827811.
13. Lu Y, Lerner MB, John Qi Z, et al. Graphene-protein bioelectronic devices with wavelength-dependent photoresponse. *Appl Phys Lett*. 2012;100(3). doi:10.1063/1.3678024.
14. Lerner MB, Matsunaga F, Han GH, et al. Scalable production of highly sensitive nanosensors based on graphene functionalized with a designed G protein-coupled receptor. *Nano Lett*. 2014;14(5):2709-2714. doi:10.1021/nl5006349.
15. Lerner MB, Pan D, Gao Y, et al. Large scale commercial fabrication of high quality graphene-based assays for biomolecule detection. *Sensors Actuators, B Chem*. 2016:1-7. doi:10.1016/j.snb.2016.09.137.
16. Artiles MS, Rout CS, Fisher TS. Graphene-based hybrid materials and devices for biosensing. *Adv Drug Deliv Rev*. 2011;63(14-15):1352-1360. doi:10.1016/j.addr.2011.07.005.
17. Choi Y, Moody IS, Sims PC, et al. Single-Molecule Lysozyme Dynamics Monitored by an Electronic Circuit. *Science (80-)*. 2012;335(6066):319-324. doi:10.1126/science.1214824.
18. Goldsmith BR, Coroneus JG, Khalap VR, Kane AA, Weiss GA, Collins PG. Conductance-Controlled Point Functionalization of Single-Walled Carbon Nanotubes. *Science (80-)*. 2007;315(5808):77-81. doi:10.1126/science.1135303.
19. Kybert NJ, Han GH, Lerner MB, Dattoli EN, Esfandiar A, Charlie Johnson AT. Scalable arrays of chemical vapor sensors based on DNA-decorated graphene. *Nano Res*. 2014;7(1):95-103. doi:10.1007/s12274-013-0376-9.
20. Gao L, Ren W, Xu H, et al. Repeated growth and bubbling transfer of graphene with millimetre-size single-crystal grains using platinum. *Nat Commun*. 2012;3:699. doi:10.1038/ncomms1702.
21. Hughes LJ, Goldstein J, Pohl J, et al. A highly specific monoclonal antibody against monkeypox virus detects the

heparin binding domain of A27. *Virology*. 2014;464-465(1):264-273. doi:10.1016/j.virol.2014.06.039.